Time-dependent Particle Densities in Finite Particle Deposition Systems

SJOERT FLEURKE
Radio Communications Agency
Emmasingel 1, 9746 AB, Groningen
THE NETHERLANDS
sjoert.fleurke@agentschaptelecom.nl

AERNOUT VAN ENTER
Johann Bernoulli Institute
University of Groningen
Nijenborg 9, 9747 AG, Groningen
THE NETHERLANDS
a.c.d.van.enter@rug.nl

Abstract: This paper contains calculations of the time-dependent particle densities in multi-layer particle deposition systems without screening. Several calculation methods are used. These methods can be used to calculate densities in all layers and are demonstrated with a number of examples. The densities in deposition systems of size 3 and 5 are calculated up to the third layer. It is also proven that border sites tend to have a higher density than sites in the middle. This partly explains why finite-sized systems tend to reach higher packing densities in higher layers than in low layers.

Key–Words: Car parking, particle deposition, random sequential adsorption, sequential frequency assignment process, multi-layer parking model

1 Introduction

Consider a lattice $\mathbb{L}(x, r)$ consisting of sites (x, r) with positions $x \in \{0, 1, 2, \ldots, n+1\}$ and heights $r \in \mathbb{N}^+$. Throughout the deposition process particles arrive according to independent Poisson processes $N_t(x)$ i.e. $P(N_t(x) = n) = t^n e^{-t}/n!$. At the border sites 0 and $n+1$ no particles arrive i.e. $N_t(0) = N_t(n+1) = 0, \forall_{t \geqslant 0}$. When a particle arrives in the system it searches vertically for the lowest available vertex. A vertex is available for the deposition of a particle if both itself and its neighboring vertices are not occupied yet. Therefore, the horizontal distance between two particles will always be at least 2. During the process the particles pile up in the system. For an example see Fig. 1.

More formally, our model can be represented as follows.

1. The state-space is $\mathbb{F} := (\mathbb{L}, \mathbb{N}^+)^{\{0,1\}}$.
2. The process $\kappa_t(x, r) = 1$ if there is a particle at (x, r) at time t and 0 otherwise.
3. A particle arriving at site x at time t, will be deposited at $h_t(x) = \min\{r : \kappa_t(y, r) = 0, \forall_{y \in N_x}\}$, with N_x the set of horizontally adjacent sites of x.

Note that this model is without the *screening* or *Tetris* feature [1]. In the model with screening particles tend to drop on top of earlier arrived particles and, contrary to the model used here, they cannot pass them in search of spaces in lower layers.

In this paper we focus on the densities of sites (or vertices). We call $\rho_t^{(x,r)}$ the density of site $(x, r) \in \mathbb{L}$ which is defined as the expectation of the occupancy of that site at time t. In other words, $\rho_t^{(x,r)} = \mathbb{E}\kappa_t(x, r)$. The end-density of a site is its long-term density and is denoted by $\rho_\infty^{(x,r)}$.

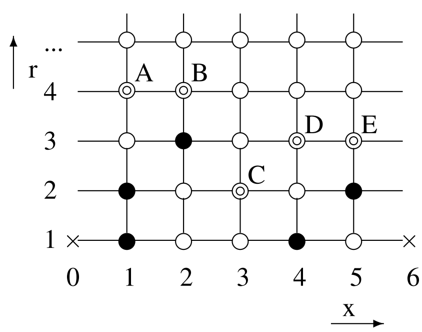

Figure 1: Parking lattice consisting of $n = 5$ positions where parking is allowed. In this example five particles have already arrived at positions 1, 2, 4 and 5. The next particle will be deposited at one of the marked positions indicated with A, B, C, D or E depending on the x-position where they arrive. The '$\times$' symbols at 0 and $n+1$ indicate that at those x-positions no particles will arrive.

The deposition model discussed in this paper is related to the Car Parking Model introduced by Rényi in 1958 [2]. In this model particles (or cars) were dropped on a single continuous line. Later discrete and multi-layer versions of the car parking process were created to model random sequential adsorption [3] [4] [5]. Higher-dimensional versions of the model have been studied as well. For example, in [6] the sequential frequency assignment process (SFAP) is studied using a continuous, multi-layer disk parking model. Recently there is growing attention among researchers for these models [7] [8] [9] [10] [11] [12] [13] [14], one of the reasons being that they can be used to study wireless network behavior.

Most analytical results concerning this model apply only to mono- or two-layer versions [5] [15] [16] [17]. The multi-layer versions of the particle deposition model are more challenging and therefore still many results are based on simulations [4] [6].

In this paper, some unpublished results from [18] are further developed. We continue the work on calculating the particle densities in small multi-layer parking models. We will calculate some particle densities on finite-sized multi-layer particle deposition systems.

In [19] a general formula was given for the densities of the center site in a system of size $n = 3$. Here we extend this work and calculate the densities of the border sites of the first two layers. Next we calculate the densities of the center sites of the system with $n = 5$.

Finally, we give general formulas for the calculation of the center and border sites deposition densities at the first layer. We use this result to prove that the average density of the border site at the first layer grows higher than that of the site in the center. This result is expected to occur on higher layers too and is further support for the theory that explains the interesting phenomenon of growing layer end-densities.

2 Notation and Definitions

For the purpose of this paper the following definitions and notations are used.

Definition 1 *The one-sided densities $f_t^{(n)}(.)$ and the pre-image motives $D_t^{(i,n)}(.)$ of a particle system of size $n \times L$ are given by*

$$\begin{aligned} f_t^{(n)}(s_1, \ldots, s_k) &= P_t(m_1 = s_1, \ldots \\ &\ldots, m_k = s_k \mid N_t(0) = 0, N_t(n+1) = 0) \quad (1) \\ D_t^{(i,n)}(s_i, \ldots, s_{i+l}) &= P_t(m_i = s_i, \ldots \\ &\ldots, m_{i+l} = s_{i+l} \mid N_t(0) = 0, N_t(n+1) = 0) \quad (2) \end{aligned}$$

where $s_i \in \{0, 1, \ldots\}$ and $N_t(j)$ denotes the Poisson counting process of particle arrivals at site j and m_j is defined as

$$m_j(t) = \sum_{i=1}^{L} 2^{i-1} 1_{\textit{layer } i \textit{ is occupied at site } j}(t) \quad (3)$$

where L is the maximum layer that is regarded in the calculation. The lattice $\mathbb{L}$ itself may have an infinite number of layers regardless of the value of L.

Note that $f_t^{(n)}(s_1, \ldots s_k) = D_t^{(1,n)}(s_1, \ldots, s_k)$.

The $f_t^{(n)}$'s and $D_t^{(i,n)}$'s are useful tools for the calculation of densities. For example, take a look at Fig. 1. If we were interested in calculating the probability of the occurrence of exactly this pattern of particles (or "image") at time t we can make a list of all the pre-image motives that may lead to the image of Fig. 1. In this particular case there are two pre-image motives which are displayed in Fig. 2 and Fig. 3.

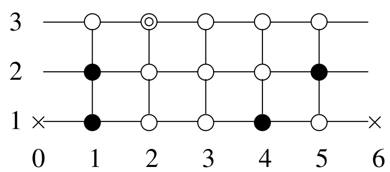

Figure 2: Pre-image motive $D_t^{(1,5)}(3, 0, 0, 1, 2)$. An arrival at position 2 will cause a desirable transition to the pattern of Fig. 1.

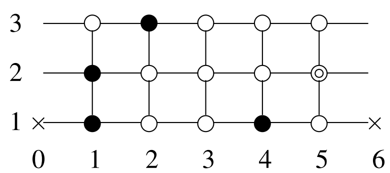

Figure 3: Pre-image motive $D_t^{(1,5)}(3, 4, 0, 1, 0)$. An arrival at position 5 will cause a desirable transition to the pattern of Fig. 1.

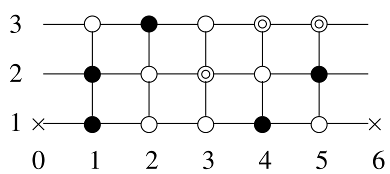

Figure 4: The image of Fig. 1 itself ($D_t^{(1,5)}(3, 4, 0, 1, 2)$) has a negative impact on its own occurrence. An arrival at one of the positions 3, 4 or 5 will cause a transition to another pattern. It should be clear that eventually this pattern will die out.

Furthermore, the occurrence of the pattern in Fig. 1 itself will eventually disappear. This is also to be taken into account (see Fig. 4).

We can now formulate the following formula for the derivative of $D_t^{(1,5)}(3,4,0,1,2)$.

$$\begin{aligned}\dot{D}_t^{(1,5)}(3,4,0,1,2) &= D_t^{(1,5)}(3,0,0,1,2)\\ &+ D_t^{(1,5)}(3,4,0,1,0)\\ &- 3D_t^{(1,5)}(3,4,0,1,2) \quad (4)\end{aligned}$$

When the pre-image motives on the right-hand side are known it is possible to solve this equation using standard techniques.

The method demonstrated here will be used extensively in the remainder of this paper.

3 Results

The following theorem concerning one-sided densities is important for the greater part of the calculations in this section.

Theorem 2 *In the case* $L = 2$ *the vector* $f_t^{(n)} = (f_t^{(n)}(0), f_t^{(n)}(1), f_t^{(n)}(2), f_t^{(n)}(1,0))^t$, $n \geqslant 1$ *obeys the linear ODE*

$$\begin{aligned}\dot{f}_t^{(n+1)}(0) &= -f_t^{(n)}(0)e^{-t} - f_t^{(n)}(1)e^{-t}\\ &\quad -f_t^{(n)}(2)e^{-t} \quad (5)\\ \dot{f}_t^{(n+1)}(1) &= f_t^{(n)}(0)e^{-t} + f_t^{(n)}(2)e^{-t}\\ &\quad -f_t^{(n+1)}(1,0) \quad (6)\\ \dot{f}_t^{(n+1)}(2) &= f_t^{(n)}(1)e^{-t} \quad (7)\\ \dot{f}_t^{(n+1)}(1,0) &= f_t^{(n)}(0)e^{-t}\\ &\quad -\left(f_t^{(n-1)}(0) + f_t^{(n-1)}(1)\right)\\ &\quad \times te^{-2t} - f_t^{(n+1)}(1,0) \quad (8)\end{aligned}$$

with initial conditions $f_0^{(n)} = (f_0^{(n)}(0), f_0^{(n)}(1), f_0^{(n)}(2), f_0^{(n)}(1,0))^t = (1,0,0,0)^t$.

Proof: Confer Theorem 6 in [17] which is a special case of this Theorem with n infinitely large. Since this special case was already proven there, it is sufficient here to show that the system of the left hand side of these equations contains 1 position less than the system on the right hand side. This is straightforward from the proof provided in [17]. Therefore we demonstrate here only the proof for the case of equation (7).

$$\begin{aligned}\dot{f}_t^{(n+1)}(2) &= \dot{P}_t^{(n+1)}(m_1 = 2) \quad (9)\\ &= P_t^{(n+1)}(m_1 = 0, m_2 = 1) \quad (10)\\ &= P_t^{(n+1)}(m_1 = 0, m_2 = 1\\ &\quad |N_t(0) = 0)P(N_t(0) = 0) \quad (11)\\ &= P_t^{(n+1)}(m_1 = 1|N_t(0) = 0)e^{-t} \quad (12)\\ &= P_t^{(n)}(m_1 = 1)e^{-t} \quad (13)\\ &= f_t^{(n)}(1)e^{-t} \quad (14)\end{aligned}$$

Notice that the transition to the system with n positions took place between equation (12) and (13). $\square$

The significance of Theorem 2 is that we can now create the one-sided density functions of arbitrarily large systems using those of smaller systems. For the purpose of this paper we provide below the results of the cases $n = 1$, $n = 2$ and $n = 3$.

It can easily checked by hand that

$$f_t^{(1)} = \begin{pmatrix} f_t^{(1)}(0)\\ f_t^{(1)}(1)\\ f_t^{(1)}(2)\\ f_t^{(1)}(1,0)\end{pmatrix} = \begin{pmatrix} e^{-t}\\ te^{-t}\\ 0\\ te^{-t}\end{pmatrix} \quad (15)$$

For example, in a system with only one position the probability that 0 particles are on the first and second layer means simply that there have been no arrivals at all. Therefore $f_t^{(1)}(0) = P(N_t(1) = 0) = e^{-t}$, etc. Starting with these $f_t^{(1)}$'s all the $f_t^{(2)}$'s are calculated using Theorem 2. This yields

$$f_t^{(2)} = \begin{pmatrix} \frac{1}{4} + \frac{3}{4}e^{-2t} + \frac{1}{2}te^{-2t}\\ \frac{1}{4} - \frac{1}{4}e^{-2t} + \frac{1}{2}te^{-2t}\\ \frac{1}{4} - \frac{1}{4}e^{-2t} - \frac{1}{2}te^{-2t}\\ te^{-2t}\end{pmatrix} \quad (16)$$

Applying Theorem 2 again on $f_t^{(2)}$ gives

$$f_t^{(3)} = \begin{pmatrix} \frac{1}{9} + \frac{3}{4}e^{-t} + \frac{5}{36}e^{-3t} + \frac{1}{6}te^{-3t}\\ \frac{8}{27} - \frac{1}{4}e^{-t} + \frac{1}{4}te^{-t} - \frac{5}{108}e^{-3t}\\ +\frac{13}{36}te^{-3t} + \frac{1}{6}t^2e^{-3t}\\ \frac{2}{9} - \frac{1}{4}e^{-t} + \frac{1}{36}e^{-3t} - \frac{1}{6}te^{-3t}\\ \frac{1}{4}te^{-t} + \frac{3}{4}te^{-3t} + \frac{1}{2}t^2e^{-3t}\end{pmatrix} \quad (17)$$

3.1 The Particle Deposition System with 3 Vertices

In this section the densities of the particle system of size $n = 3$ are calculated for the first three layers using the results above. For reasons of symmetry it suffices to calculate the densities $\rho_t^{(1,3)}(1)$ and $\rho_t^{(2,3)}(1)$ at layer 1, $\rho_t^{(1,3)}(2)$ and $\rho_t^{(2,3)}(2)$ at layer 2, and $\rho_t^{(1,3)}(3)$ and $\rho_t^{(2,3)}(3)$ at layer 3.

Let us first focus on the densities at the border sites. Obviously, for the first two layers we can use the result of $f_t^{(3)}$ in (17) because $\rho_t^{(1,3)}(1) = f_t^{(3)}(1) + f_t^{(3)}(3)$ and $\rho_t^{(1,3)}(2) = f_t^{(3)}(2) + f_t^{(3)}(3)$. Therefore, we have

$$\begin{aligned}
\rho_t^{(1,3)}(1) &= f_t^{(3)}(1) + f_t^{(3)}(3) && (18)\\
&= f_t^{(3)}(1) + \int_0^t f_u^{(3)}(1,0)du && (19)\\
&= \frac{8}{27} - \frac{1}{4}e^{-t} + \frac{1}{4}te^{-t} - \left(\frac{5}{108}\right.\\
&+ \left.\frac{13}{36}t + \frac{1}{6}t^2\right) e^{-3t}\\
&+ \frac{10}{27} - \frac{1}{4}e^{-t} - \frac{1}{4}te^{-t} - \left(\frac{13}{108}\right.\\
&\left.+\frac{39}{108}t + \frac{1}{6}t^2\right) e^{-3t} && (20)\\
&= \frac{2}{3} - \frac{1}{2}e^{-t} - \frac{1}{6}e^{-3t} && (21)
\end{aligned}$$

The particle density $\rho_t^{(1,3)}(2)$ can be calculated similarly and this yields.

$$\begin{aligned}
\rho_t^{(1,3)}(2) &= \frac{16}{27} - \frac{1}{2}e^{-t} - \frac{1}{4}te^{-t}\\
&- \left(\frac{5}{54} + \frac{19}{36}t + \frac{1}{6}t^2\right) e^{-3t} && (22)
\end{aligned}$$

Let us now calculate the densities at the center site. Here too the one-sided densities are of help. The derivatives of these functions can be expressed in terms of pre-image motives as below.

$$\begin{aligned}
\dot{\rho}_t^{(2,3)}(1) &= D_t^{(1,3)}(0,0,0) && (23)\\
\dot{\rho}_t{}^{(2,3)}(2) &= 2D_t^{(1,3)}(0,0,1)\\
&+D_t^{(1,3)}(1,0,1) + D_t^{(1,3)}(0,1,0) && (24)\\
\dot{\rho}_t^{(2,3)}(3) &= 2D_t^{(1,3)}(0,0,3) + 2D_t^{(1,3)}(1,0,3)\\
&+D_t^{(1,3)}(3,0,3) + 2D_t^{(1,3)}(0,1,2)\\
&+D_t^{(1,3)}(2,1,2) + 2D_t^{(1,3)}(0,2,1)\\
&+D_t^{(1,3)}(1,2,1) + D_t^{(1,3)}(0,3,0) && (25)
\end{aligned}$$

The quantities of the form $D_t^{(1,3)}(x,0,y)$, with $x, y \in \{0,1,3,7\}$ can be calculated directly using

$$D_t^{(k,n)}(x,0,y) = f_t^{(k)}(x)f_t^{(k)}(y)e^{-t} \qquad (26)$$

The one-sided densities with $k = 1$ can be written down immediately as they follow from the definition of the Poisson process, i.e.

$$\begin{aligned}
f_t^{(1)}(0) &= e^{-t} && (27)\\
f_t^{(1)}(1) &= te^{-t} && (28)\\
f_t^{(1)}(3) &= \frac{t^2}{2}e^{-t} && (29)\\
f_t^{(1)}(7) &= 1 - e^{-t} - te^{-t} - \frac{t^2}{2}e^{-t} && (30)
\end{aligned}$$

The other D_t's can be calculated using the following differential equations

$$\begin{aligned}
\dot{D}_t^{(1,3)}(0,1,0) &= D_t^{(1,3)}(0,0,0)\\
&- 3D_t^{(1,3)}(0,1,0)\\
\dot{D}_t^{(1,3)}(0,1,2) &= D_t^{(1,3)}(0,1,0)\\
&- 3D_t^{(1,3)}(0,1,2)\\
\dot{D}_t^{(1,3)}(2,1,2) &= 2D_t^{(1,3)}(0,1,2)\\
&- 3D_t^{(1,3)}(2,1,2)\\
\dot{D}_t^{(1,3)}(0,2,1) &= D_t^{(1,3)}(0,0,1) && (31)\\
&- 3D_t^{(1,3)}(0,2,1)\\
\dot{D}_t^{(1,3)}(1,2,1) &= D_t^{(1,3)}(1,0,1)\\
&+ 2D_t^{(1,3)}(0,2,1)\\
&- 3D_t^{(1,3)}(1,2,1)\\
\dot{D}_t^{(1,3)}(0,3,0) &= D_t^{(1,3)}(0,1,0)\\
&- 3D_t^{(1,3)}(0,3,0)
\end{aligned}$$

Solving these equations is straightforward and results in

$$\begin{aligned}
D_t^{(1,3)}(0,1,0) &= te^{-3t} && (32)\\
D_t^{(1,3)}(0,1,2) &= t^2e^{-3t}/2 && (33)\\
D_t^{(1,3)}(2,1,2) &= t^3e^{-3t}/3 && (34)\\
D_t^{(1,3)}(0,2,1) &= t^2e^{-3t}/2 && (35)\\
D_t^{(1,3)}(1,2,1) &= 2\,t^3e^{-3t}/3 && (36)\\
D_t^{(1,3)}(0,3,0) &= t^2e^{-3t}/2 && (37)
\end{aligned}$$

Solving (23)-(25) with the use of (26) and the solutions (32)-(37), gives the following average densities in the first 3 layers.

$$\rho_t^{(2,3)}(1) = \frac{1}{3} - \frac{1}{3}e^{-3t} \quad (38)$$

$$\rho_t^{(2,3)}(2) = \frac{11}{27} - \left(\frac{11}{27} + \frac{11}{9}t + \frac{1}{3}t^2\right)e^{-3t} \quad (39)$$

$$\begin{aligned}\rho_t^{(2,3)}(3) &= \frac{35}{81} - \left(\frac{35}{81} + \frac{35}{27}t + \frac{35}{18}t^2\right. \\ &\quad \left. + \frac{7}{9}t^3 + \frac{1}{12}t^4\right)e^{-3t} \quad (40)\end{aligned}$$

In [19] the same results were found through the use of a general formula for the center sites at all layers of a system with 3 positions.

3.2 The Particle Deposition System with 5 Vertices

The densities at layer one and two of the center site $(3,5)$ obey the differential equations

$$\begin{aligned}\dot{\rho}_t^{(3,5)}(1) &= D_t^{(2,5)}(0,0,0) \\ &\quad + 2D_t^{(2,5)}(0,0,2) + D_t^{(2,5)}(2,0,2) \quad (41) \\ \dot{\rho}_t^{(3,5)}(2) &= 2D_t^{(2,5)}(0,0,1) + D_t^{(2,5)}(1,0,1) \\ &\quad + D_t^{(2,5)}(0,1,0) \quad (42)\end{aligned}$$

The densities of the form $D_t^{(2,5)}(x,0,y)$, with $x,y \in \{0,1,2\}$ can be calculated directly using equation (26) and vector $f_t^{(2)}$. The density $D_t^{(2,5)}(0,1,0)$ will be treated separately.

$$\begin{aligned}D_t^{(2,5)}(0,0,0) &= \frac{9}{16}e^{-5t} + \frac{3}{8}e^{-3t} \\ &+ \frac{1}{16}e^{-t} + \frac{3}{4}e^{-5t}t \\ &+ \frac{1}{4}e^{-3t}t + \frac{1}{4}e^{-5t}t^2 \quad (43) \\ D_t^{(2,5)}(0,0,1) &= -\frac{3}{16}e^{-5t} + \frac{1}{8}e^{-3t} \\ &+ \frac{1}{16}e^{-t} + \frac{1}{4}e^{-5t}t \\ &+ \frac{1}{4}e^{-3t}t + \frac{1}{4}e^{-5t}t^2 \quad (44) \\ D_t^{(2,5)}(1,0,1) &= \frac{1}{16}e^{-5t} - \frac{1}{8}e^{-3t} \\ &+ \frac{1}{16}e^{-t} - \frac{1}{4}e^{-5t}t \\ &+ \frac{1}{4}e^{-3t}t + \frac{1}{4}e^{-5t}t^2 \quad (45)\end{aligned}$$

$$\begin{aligned}D_t^{(2,5)}(0,0,2) &= -\frac{3}{16}e^{-5t} + \frac{1}{8}e^{-3t} \\ &+ \frac{1}{16}e^{-t} - \frac{1}{2}e^{-5t}t \\ &- \frac{1}{4}e^{-5t}t^2 \quad (46) \\ D_t^{(2,5)}(2,0,2) &= \frac{1}{16}e^{-5t} - \frac{1}{8}e^{-3t} \\ &+ \frac{1}{16}e^{-t} + \frac{1}{4}e^{-5t}t \\ &- \frac{1}{4}e^{-3t}t + \frac{1}{4}e^{-5t}t^2 \quad (47)\end{aligned}$$

Solving equation (41) and using $\rho_0^{(3,5)}(1) = 0$ results in

$$\rho_t^{(3,5)}(1) = \frac{7}{15} - \frac{1}{4}e^{-t} - \frac{1}{6}e^{-3t} - \frac{1}{20}e^{-5t} \quad (48)$$

For the calculation of the density on the second layer it is necessary to calculate $D_t^{(2,5)}(0,1,0)$ as well. The following differential equation has to be solved.

$$\begin{aligned}\dot{D}_t^{(2,5)}(0,1,0) &= D_t^{(2,5)}(0,0,0) \\ &- D_t^{(2,5)}(0,1,0) \\ &- 2D_t^{(2,5)}(0,1,0,0) \\ &- 2D_t^{(2,5)}(0,1,0,1)\end{aligned} \quad (49)$$

It is easy to see that

$$\begin{aligned}D_t^{(2,5)}(0,1,0,0) &= f_t^{(2)}(0,1)f_t^{(1)}(0)e^{-t} \quad (50) \\ D_t^{(2,5)}(0,1,0,1) &= f_t^{(2)}(0,1)f_t^{(1)}(1)e^{-t} \quad (51)\end{aligned}$$

So we can now solve (49) immediately. It has the solution

$$\begin{aligned}D_t^{(3,5)}(0,1,0) &= \frac{1}{32}(7+2t)e^{-t} \\ &- \frac{1}{16}\left(1-8t-4t^2\right)e^{-3t} \\ &- \frac{5}{32}\left(1-6t-4t^2\right)e^{-5t}\end{aligned} \quad (52)$$

Knowing the expressions for $D_t^{(2,5)}(0,0,1)$, $D_t^{(2,5)}(1,0,1)$, and $D_t^{(2,5)}(0,1,0)$, (42) can be solved as well using the usual techniques.

For the densities in the first and second layer of the vertex in the center it follows that

$$\begin{aligned}\rho_t^{(3,5)}(1) &= \frac{7}{15} - \frac{1}{4}e^{-t} - \frac{1}{6}e^{-3t} \\ &- \frac{1}{20}e^{-5t} \end{aligned} \quad (53)$$

$$\begin{aligned}\rho_t^{(3,5)}(2) &= \frac{46823}{108000} - \frac{407219}{2160000}e^{-t} \\ &- \frac{1}{16}te^{-t} - \frac{3}{16}e^{-2t} \\ &- \frac{1}{8}te^{-2t} - \frac{1}{36}e^{-3t} \\ &- \frac{5}{24}te^{-3t} - \frac{79}{864}e^{-4t} \\ &- \frac{13}{72}te^{-4t} - \frac{1}{12}t^2e^{-4t} \\ &+ \frac{1429}{16000}e^{-5t} - \frac{49}{800}te^{-5t} \\ &- \frac{11}{80}t^2e^{-5t} - \frac{7457}{270000}e^{-6t} \\ &- \frac{847}{9000}te^{-6t} - \frac{31}{300}t^2e^{-6t} \\ &- \frac{1}{30}t^3e^{-6t} \end{aligned} \quad (54)$$

The limiting densities are close to each other: $\frac{7}{15} \approx 0.467 > \frac{46823}{108000} \approx 0.434$. Apparently, in the system with $n = 5$ positions the density of the center vertex is slightly lower in the second layer than in the first layer. This is contrary to the situation in the system with infinite positions [17] and the system with 3 positions as can be checked by comparing (38) and (39).

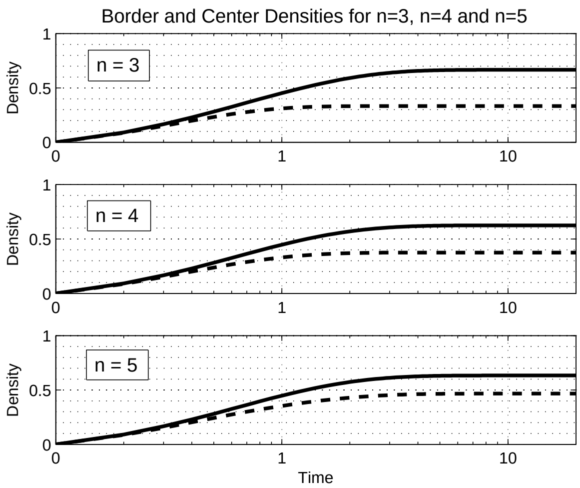

Figure 5: Particle densities at the border and in the center of the deposition systems of several sizes as calculated with the methods demonstrated in this paper. The higher lines represent the development of the border site densities in time. The fact that center densities are dominated by the border densities as proven in Theorem 4. Note however that the difference decreases for larger systems.

3.3 Relations between vertex densities at the first layer

Lemma 3 *Consider a parking system with n vertices. During the particle deposition process the center vertex at the first layer $(m, 1)$ has the particle density*

$$\rho_t^{(m,n)}(1) = \int_0^t [f_u^{(m-1)}(0)]^2 e^{-u} du \quad (55)$$

if $n = 2m - 1$, or

$$\rho_t^{(m,n)}(1) = \int_0^t f_u^{(m-1)}(0) f_u^{(m)}(0) e^{-u} du \quad (56)$$

if $n = 2m$. The border vertex $(1, 1)$ has the particle density

$$\rho_t^{(1,n)}(1) = \int_0^t f_u^{(n-1)}(0) e^{-u} du \quad (57)$$

This result was earlier reported in a slightly different form by Cohen and Reiss [5]. The proof is straightforward.

Proof: Let $(x, 1), x \in \{1, 2, \ldots, N\}$ be a vertex on lattice $\mathbb{L}$. The density on site x may increase only if the site itself and its neighbors are free, therefore we have

$$\begin{aligned}\dot{\rho}_t^{(x,n)}(1) = D_t^{(1,n)}(&v_1, v_2, \ldots \\ &\ldots, v_{x-2}, 0, 0, 0, v_{x+2}, \ldots, v_n) \end{aligned} \quad (58)$$

where v_i can be 0 or 1. Notice that the value of v_x and its neighbors must be 0 which means that there were no arrivals in v_x at all. But in that case the developments at the left side of x are independent of the developments at the right side. Therefore we may continue with

$$\begin{aligned}\dot{\rho}_t^{(x,n)}(1) &= D_t^{(1,x-1)}(v_1, \ldots, v_{x-2}, 0) \\ &\times P(N_t(x) = 0) \\ &\times D_t^{(1,n-x+1)}(0, v_2, \ldots, v_{n-x+1}) \quad (59) \\ &= f_t^{(x-1)}(0) f_t^{(n-x+1)}(0) e^{-t} \quad (60) \end{aligned}$$

Taking the integral on both sides and applying suitable values for x and n yields the results of the lemma. □

Theorem 4 *The density in the center vertex is lower than the density in a border vertex.*

$$\rho_t^{(x,2x-1)}(1) < \rho_t^{(1,2x-1)}(1) \quad (61)$$

Proof: For the purpose of this proof we will use the short-hand notation $f_m = f_t^{(m)}(0)$. From lemma 3 we know that $\dot{\rho}_t^{(m,n)}(1) = f_{(m-1)}^2 e^{-t}$. From simulation results we know that the end-density of border vertices on the first layer typically lies between $1/2$ to $2/3$ depending on the size of the system. In any case, suppose $\rho^{(1,m-1)} = \rho^{(1,2m-2)} + d$, for some d. Then we may write

$$\begin{aligned}
\dot{\rho}_t^{(m,2m-1)}(1)e^t &= f_{(m-1)}^2 && (62)\\
&= (1-\rho_t^{(1,m-1)})^2 && (63)\\
&= (1-(\rho_t^{(1,2m-2)}+d))^2 && (64)\\
&= 1-2(\rho_t^{(1,2m-2)}+d)\\
&+ (\rho_t^{(1,2m-2)}+d)^2 && (65)\\
&= 1-\rho_t^{(1,2m-2)}\\
&+ \rho_t^{(1,2m-2)}(\rho_t^{(1,2m-2)}+d)\\
&- \rho_t^{(1,2m-2)}\\
&+ d(\rho_t^{(1,2m-2)}+d)-d && (66)\\
&= 1-\rho_t^{(1,2m-2)}\\
&- \rho_t^{(1,2m-2)}(1-\rho_t^{(1,m-1)})\\
&- d(1-\rho_t^{(1,m-1)}) && (67)\\
&= 1-\rho_t^{(1,2m-2)}\\
&- \rho_t^{(1,m-1)}(1-\rho_t^{(1,m-1)})\\
&\leqslant 1-\rho_t^{(1,2m-2)} && (68)\\
&= f_{(2m-2)} && (69)
\end{aligned}$$

So, we have

$$\begin{aligned}
\dot{\rho}_t^{(m,2m-1)}(1) &\leqslant f_{(2m-2)}e^{-t} && (70)\\
&= \dot{\rho}_t^{(1,2m-1)}(1) && (71)
\end{aligned}$$

It follows that the density of a border site grows faster and reaches a higher value than the site in the center. For the case $n = 2m$ this proof is similar. □

This result should not be surprising. In finite-sized systems particles at border sites have only one neighboring site while all others have two neighbors. Therefore a particle arriving at the border is more likely to be accepted in the first layer than particles arriving in the center.

Although not proven here, it is logical to assume that the same applies to the second layer and higher. After a while this would result in a lower maximum height at the border sites. Then newly arriving particles at the sites next to the border will only see neighbors on one side instead of two when they arrive, etcetera. Eventually it becomes increasingly unlikely that gaps of size 2 are created, which implies a higher particle density. This is exactly what our simulations have shown [19].

4 The Particle Deposition System with Screening

The model discussed in this paper is not to be confused with the deposition model with screening. In the model with screening particles are not capable of passing through layers that have no space for them. This results in a lower layer-density compared with the model without screening treated here. In our earlier work we reported about some properties of the model with screening [20]. One result was that the density of higher layers tends to

$$\lim_{r,t\to\infty} \rho_t^{(2,3)}(r) = \frac{1}{2+\frac{1}{5}\sqrt{5}} \approx 0.408628 \qquad (72)$$

while in the model without screening it was proven [19] that the value of the end-density goes to exactly $\frac{1}{2}$.

Unfortunately, in the same paper, the section about the densities on the first 3 layers contains an error. Below are the correct formulas of the densities for the first 3 layers of the center vertex.

$$\begin{aligned}
\rho_t^{(2,3)}(1) &= \frac{1}{3}-\frac{1}{3}e^{-3t} && (73)\\
\rho_t^{(2,3)}(2) &= \frac{11}{27}-\left(\frac{11}{27}+\frac{11}{9}t+\frac{1}{3}t^2\right)e^{-3t} && (74)\\
\rho_t^{(2,3)}(3) &= \frac{11}{27}-\left(\frac{11}{27}+\frac{11}{9}t++\frac{11}{6}t^2\right.\\
&\left.+\frac{2}{3}t^3+\frac{1}{12}t^4\right)e^{-3t} && (75)
\end{aligned}$$

Note that at the first two layers the densities for the model with and without screening are exactly the same. This is not surprising because the screening feature at a system with only 3 positions is not able to block arrivals in the center of the first two layers.

5 Conclusion

The results in this paper show that it is possible to calculate time-dependent particle densities in finite-sized particle deposition systems. Sometimes it is even possible to choose between several techniques. However, the calculation of densities of sites in higher layers requires, even in relatively small systems, an increasing effort. It was also proven that border sites have a larger chance to be filled than sites near the center. Simulations have shown an increasing layer end-density. Lower layers are less dense packed than higher layers. The mechanism behind it is believed to be understood but proving this analytically remains a challenge.

References:

[1] S.R. Fleurke, C. Külske, Multilayer Parking with Screening on a Random Tree, *J. Stat. Phys.* 139, no.3, 2010, pp. 417–431.

[2] A. Rényi, On a One-dimensional Problem Concerning Random Space-filling, *Publ. Math. Inst. Hung. Acad. Sci.* 3, 1958, pp. 109–127.

[3] J.W. Evans, Random and Cooperative Sequential Adsorption, *Rev. Mod. Phys.* 64, no. 4, 1993, pp. 1281–1327.

[4] P. Nielaba, V. Privman, Multilayer Adsorption with Increasing Layer Coverage, *Phys. Rev.* A 45, 1992, pp. 6099–6102.

[5] R. Cohen, H. Reiss, Kinetics of Reactant Isolation I. *One-Dimensional Problems, J. Chem. Phys.* 38, no. 3, 1963, pp. 680–691.

[6] H.G. Dehling, S.R. Fleurke, The Sequential Frequency Assignment Process *Proc. of the 12th WSEAS Internat. Conf. on Appl. Math., Cairo, Egypt*, 2007, pp. 280–285.

[7] R. Gouet, A. Sudbury, Blocking and Dimer Processes on the Cayley Tree, *J. Stat. Phys.* 130, no. 5, 2008, pp. 935–955.

[8] S. Dhara, J.S.H. van Leeuwaarden, D. Mukherjee, Generalized Random Sequential Adsorption on Sparse Random Graphs, (Submitted on 13 Apr. 2016. arXiv:1604.03918)

[9] M.D. Penrose, A. Sudbury, Exact and approximate results for deposition and annihilation processes on graphs, *Ann. Appl. Prob.* 15, no. 1B, 2005, pp. 853–889.

[10] C.J.E. Daniels, M.D. Penrose, Percolation of even sites for enhanced random sequential adsorption, (Submitted on 31 Aug. 2015. arXiv:1508.07965)

[11] V. Privman, H. Yan, Random Sequential Adsorption on Imprecise Lattice (Submitted on 6 Jun. 2016. arXiv:1606.01823)

[12] N.I. Lebovka, Y.Yu. Tarasevich, D.O. Dubinin, V.V. Laptev, N.V. Vygornitskii, Jamming and percolation in generalized models of random sequential adsorption of linear k-mers on a square lattice, *Phys. Rev. E* 92, 2015.

[13] T.S. Mountford, A. Sudbury, Deposition processes with hardcore behavior, *J. Stat. Phys.* 146, no. 4, 2012, pp. 687–700.

[14] P. Bermolen, M. Jonckheere, F. Larroca, P. Moyal. Estimating the spatial reuse with configuration models. (arXiv:1411.0143, 2014)

[15] P.C. Hemmer, The Random Parking Problem, *J. Stat. Phys.* 57, 1989, pp. 865–869.

[16] H.G. Dehling, S.R. Fleurke, C. Külske, Parking on a Random Tree, *J. Stat. Phys.* 133, no. 1, 2008, pp. 151–157.

[17] S.R. Fleurke, C. Külske, A Second-row Parking Paradox, *J. Stat. Phys.* 136, no. 2, 2009, pp. 285–295.

[18] S.R. Fleurke, *Stochastic models for particle deposition, car parking and frequency assignment*, (Groningen Thesis), 2011, pp. 40–43.

[19] S.R. Fleurke, A.C.D. van Enter, Analytical Results for a Small Multilayer Parking System, in *Computational Problems in Engineering*. V. Mladenov, N. Mastorakis, eds., Switzerland, Springer International Publishing, 2014, pp. 43–53.

[20] S.R. Fleurke, A.C.D. van Enter, Multiple-layer parking with screening, *Proc. of the 2015 Int. Conf. on Pure Math., Appl. Math. and Comp. Meth. (PMAMCM 2015)* Recent Advances in Mathematics, 2015, pp. 22–26.